JOURNAL OF
Materials
CHEMISTRY

Studies of the thermal and photochemical decomposition mechanisms of $\mathrm{Bu^t_2Se}$ in the presence or absence of $\mathrm{Me_2Zn}$ using deuterium labelled analogues

Nigel L. Pickett,[a] Douglas F. Foster,[a] Nick Maung[b] and David J. Cole-Hamilton*[a]

[a]*School of Chemistry, University of St. Andrews, St. Andrews, Fife, Scotland, UK KY16 9ST. E-mail: djc@st-aud.ac.uk*
[b]*Advanced Materials Research Laboratories, North East Wales Institute, Plas Coch, Mold Rd., Wrexham, Wales, UK LL11 2AW*

Received 27th May 1999, Accepted 6th September 1999

Thermal decomposition of $\mathrm{Bu^t_2Se}$ in helium produces 2-methylpropene and 2-methylpropane (8 : 1) and no volatile selenium containing products, apart from the element. In hydrogen, the products are the same (8 : 1 ratio of 2-methylpropene : 2-methylpropane). However, the 2-methylpropane produced by decomposing d^{18}-$\mathrm{Bu^t_2Se}$ in H_2 contains significant amounts of hydrogen ($d^9 : d^{10} = 2.6 : 1$). In the codecomposition of d^0- and d^{18}-$\mathrm{Bu^t_2Se}$ in helium, d^0, d^1, d^9 and d^{10}-2-methylpropane are all formed, but d^9-$\mathrm{Bu^t_2Se}$ is not a product. Photolysis of d^0- and d^{18}-$\mathrm{Bu^t_2Se}$ in helium at room temperature produces 2-methylpropane and 2-methylpropene (1 : 1) with the 2-methylpropane being d^0, d^1, d^9 and d^{10}. d^9-$\mathrm{Bu^t_2Se}$ is also formed along with small amounts of 2,2,3,3-tetramethylbutane and d^0- and d^{18}-$\mathrm{Bu^t_2Se_2}$. Thermal codecomposition of $\mathrm{Me_2Zn}$ with d^{18}-$\mathrm{Bu^t_2Se}$ in H_2 produces d^0 and d^1-methane and d^8-2-methylpropene together with traces of d^8-2-methylpropane.

These results are interpreted as indicating that thermally, $\mathrm{Bu^t_2Se}$ decomposes *via* homolytic cleavage of the Se–C bonds and that the free $\mathrm{Bu^{t\cdot}}$ so formed initiates a radical chain reaction involving $H^\cdot$ as the chain carrier through its reaction with intact $\mathrm{Bu^t_2Se}$ to give hydrogen, 2 × 2-methylpropene, Se and $H^\cdot$. The chain is initiated by $\mathrm{Bu^{t\cdot}}$ abstracting $H^\cdot$ from $\mathrm{Bu^t_2Se}$ or from H_2. Semi-empirical calculations carried out with a variety of levels of theory have confirmed that E–C bond cleavage is the first step in the decomposition of all the group 16 precursors studied and have been used to model the product distribution with time. They confirm the conclusions drawn on the basis of our experimantal observations, except that the $H^\cdot$ abstraction reactions from intact $\mathrm{Bu^t_2Se}$ probably do not occur by a concerted pathway, rather they are stepwise. The radical chain process also occurs in the presence of $\mathrm{Me_2Zn}$, but the radical chain initiator in this case is $\mathrm{Me^\cdot}$ from homolytic fission of the Zn–C bonds. Evidence is presented that these reactions occur on the ZnSe surface. The small amount of 2-methylpropane produced from reaction of $\mathrm{Me_2Zn}$ with $\mathrm{Bu^t_2Se}$ in H_2 comes from hydrogenation of 2-methylpropene catalysed by ZnSe. Photochemically, homolytic cleavage of the Se–C bonds in $\mathrm{Bu^t_2Se}$ again occurs, but $\mathrm{Bu^tSe^\cdot}$ has sufficient lifetime to recombine with $\mathrm{{}^tBu^\cdot}$ and the major hydrocarbon products are formed from radical–radical reactions.

Introduction

Since we first introduced 2,2-dimethylpropanethiol(*tert*-butyl thiol, $\mathrm{Bu^tSH}$) as a sulfur precursor for growing ZnS by metal organic vapour phase epitaxy (MOVPE),[1,2] di-*tert*-butyl chalcogenides, $\mathrm{Bu^t_2E}$, and $\mathrm{Bu^tEH}$ (E = S or Se) have become widely used for MOVPE of wide band gap II–VI semiconductors, ME (M = Zn or Cd).[3–10] This is partly because the simplest system, that involving H_2E, is plagued by prereaction problems leading to the formation of nanoparticulate deposits,[11–14] partly because the $\mathrm{Bu^t}$ containing compounds are the least stable of the simple metal alkyls and have suitable volatilities and partly because attempts to dope the grown layers p-type using ammonia or amines as the sources of dopant N lead in many cases to nitrogen incorporation but much of it is not electrically active.[15] There is considerable evidence that the electrical inactivity arises because of passivation and in some cases this has been traced back to the presence of N–H which, being isoelectronic with S or Se will not be electrically active.[6,9,15] The source of the passivating hydrogen could be the amine, especially if it contains N–H initially, the ambient (growth is usually carried out in hydrogen) or the group 16 precursor. In order to remove one of the potential sources of H, researchers have tended to favour $\mathrm{Bu^t_2E}$ over $\mathrm{Bu^tEH}$, although, without detailed studies of the mechanism of decomposition of $\mathrm{Bu^t_2E}$, and of their reactions with $\mathrm{Me_2M}$, one cannot be certain that neither $\mathrm{Bu^tEH}$ nor H_2E is formed *in situ* during the decomposition. We have recently reported[16] that $\mathrm{Bu^tEH}$ react with $\mathrm{Me_2M}$ in the gas phase to give clusters, $[\mathrm{MeMEBu^t}]_5$, which further decompose *via* involatile $[\mathrm{M(EBu^t)_2}]_n$ to give nanoparticles of ME. Thus the active hydrogen atom is removed and may not be important as a passivator for dopant N.

There have been some studies which show that $\mathrm{Bu^t_2S}$ decomposes cleanly to $\mathrm{Bu^tSH}$ and 2-methylpropene and thence to H_2S and 2-methylpropene.[17–19] These are the classic products of β-H abstraction (Fig. 1) but reactions in the presence of cyclohexene have been interpreted as involving a first step that is S–C bond cleavage to give free radicals ($\mathrm{Bu^{t\cdot}}$ and $\mathrm{Bu^tS^\cdot}$).[18]

For $\mathrm{Bu^tSH}$, detailed studies of the kinetic order of the reaction and the effect of cyclohexene have been interpreted in

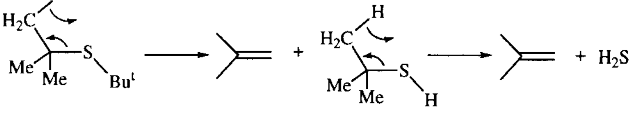

Fig. 1 β-abstraction pathway for the decomposition of $\mathrm{Bu^t_2S}$.

$$\mathrm{Bu^tSH} \rightleftharpoons \mathrm{Bu^{t\bullet}} + \mathrm{HS^{\bullet}} \qquad (1)$$

$$\mathrm{HS^{\bullet}} + \mathrm{Bu^tSH} \longrightarrow \mathrm{H_2S} + \mathrm{C_4H_8} + \mathrm{HS^{\bullet}} \qquad (2)$$

Scheme 1 Free radical process proposed for the decomposition of $\mathrm{Bu^tSH}$.[20]

terms of initial S–C bond cleavage followed by a radical chain process involving abstraction of H from the $\mathrm{Bu^t}$ group of intact $\mathrm{Bu^tSH}$ by either $\mathrm{Bu^{t\cdot}}$ or $\mathrm{HS^{\cdot}}$ (Scheme 1).[20] Later studies have generally confirmed this analysis,[18,21–24] although β-H abstraction has also been proposed.[21,24]

For $\mathrm{Bu^t_2Se}$, a marked effect of the nature of the surface over which the reaction is carried out has been noted,[25] perhaps suggesting that surface catalysed reactions may be important, but, despite not having observed $\mathrm{Bu^tSeH}$ as a product, the β-H abstraction mechanism was proposed. Against this, a possible reaction with H_2 or $\mathrm{H^{\cdot}}$ generated from the carrier gas was noted and reactions in D_2 or He ambients were suggested as ways of exploring this type of reaction. They were not, however, carried out.[25] In IR studies, we tentatively identified $\mathrm{Bu^tSeH}$ as a decomposition product of $\mathrm{Bu^t_2Se}$ and this together with preliminary theoretical calculations led us to propose that β-H abstraction was important.[26]

In view of the somewhat conflicting data especially on the decomposition pathway for $\mathrm{Bu^t_2Se}$, we have carried out detailed studies of the thermal and photochemical decomposition of $\mathrm{Bu^t_2Se}$ in a variety of different ambients (He, H_2 or D_2) as well as of $\mathrm{d^{18}}$-$\mathrm{Bu^t_2Se}$,† again in various different ambients, sometimes in the presence of $\mathrm{d^0}$-$\mathrm{Bu^t_2Se}$ and/or $\mathrm{Me_2Zn}$. We have previously shown that labelling studies of this kind can give deep insight into the precise mechanisms involved in the decomposition process of *e.g.* $\mathrm{Pr^i_2Te}$.[27] In that study, we showed that $\mathrm{Pr^i_2Te}$ decomposes by Te–C bond cleavage to give $2\times\mathrm{Pr^{i\cdot}}$ and Te. $\mathrm{Pr^{i\cdot}}$ then reacts with intact $\mathrm{Pr^i_2Te}$ to give propane, 2 × propene, Te and $\mathrm{H^{\cdot}}$, as shown in Fig. 2. Labelling studies have been used by others to help in the study of the mechanism of decomposition of primary and secondary butanethiols.[24] We also report the results of semi-empirical calculations carried out for reactions involved in the decomposition of $\mathrm{Bu^t_2Se}$ in H_2 or He. Preliminary reports of some of these results have appeared.[28,29]

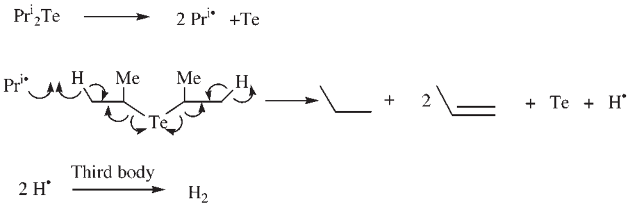

Fig. 2 Radical decomposition mechanism for $\mathrm{Pr^i_2Te}$.[27]

Experimental

General procedures

All preparations were carried out under dry oxygen free nitrogen or argon (BOC) purified by passing through two consecutive columns (2.5 cm × 80 cm) packed with $\mathrm{Cr^{2+}}$ on silica. Greaseless joints and taps were employed and manipulations were carried out using standard Schlenk line and catheter tubing techniques. The solvents, THF and pentane (Fisher Scientific UK), were dried by distillation from sodium diphenylketyl and degassed prior to use. Powdered lithium (99% with 0.5% sodium) was purchased from Aldrich. Amorphous Se powder of 99.9999% purity and particle size <325 mesh was purchased from Johnson Matthey. $\mathrm{d^9}$-$\mathrm{Bu^tCl}$ was purchased from CDN Isotopes Inc. and used as supplied. $\mathrm{Me_2Zn}$[30] and $\mathrm{Bu^t_2Se}$[31] were prepared and purified as described previously. NMR spectra were recorded on a Brüker Associates AM300 spectrometer operating in the Fourier transform mode with (for ^{13}C) noise proton decoupling. The $^{13}\mathrm{C}\{^1\mathrm{H}\}$ and ^{1}H NMR spectra were run in deuteriated solvents for the lock signal, with chemical shifts quoted in ppm to high frequency of tetramethylsilane (TMS) as the internal reference.

Preparation of $\mathrm{d^{18}}$-$\mathrm{Bu^t_2Se}$

A solution of $\mathrm{d^9}$-$\mathrm{Bu^tLi}$ (1.7 mol dm^{-3}) in pentane was prepared from the $\mathrm{Bu^tOMe}$ catalysed reaction between $\mathrm{d^9}$-$\mathrm{Bu^tCl}$ and Li according to the literature procedure.[32,33] $\mathrm{d^{18}}$-$\mathrm{Bu^t_2Se}$ was prepared as previously described for $\mathrm{Bu^t_2Se}$[31] from the dropwise addition over *ca.* 3 h of the pentane solution of $\mathrm{d^9}$-$\mathrm{Bu^tLi}$ (100 cm^3, 1.7 mol dm^{-3}, 0.17 mol) to a stirred solution of '$\mathrm{SeCl_2}$' (0.28 mol dm^{-3}, 0.084 mol) in THF (300 cm^3). This yielded 5.7 g (32%) of $\mathrm{d^{18}}$-$\mathrm{Bu^t_2Se}$ after purification. NMR (20% in $\mathrm{CH_2Cl_2}$–$\mathrm{CD_2Cl_2}$); δ_D 1.44 (s,CD$_3$); δ_C 33.2 (heptet, $J_{\mathrm{D-C}} = 19.3$ Hz, *C*D$_3$), 41.6 *C*(CD$_3$)$_3$.

Decomposition studies

The carrier gas (H_2, He or D_2) was passed through flow meters into glass bubblers containing the required precursors, which were connected to a quartz pyrolysis tube (30 cm × 2 cm diameter) held within a tube furnace so that mixing of the gas streams emanating from the bubblers occurred within the pyrolysis tube. The effluent from the pyrolysis tube was passed through stainless steel tubing to a gas sampling valve (0.5 or 1 cm^{-3}) attached to the inlet (splitless injection mode) of a capillary gas chromatograph (Hewlett Packard 5890) with mass spectrometric (Hewlett Packard 5792) detection (GCMS). Both the effluent from the GCMS and that from the bypass of the gas sampling valve were passed through activated carbon scrubbers (Embacel) and then through propan-2-ol (to remove any traces of $\mathrm{Me_2Zn}$) and aqueous $\mathrm{CuSO_4}$ solution (to remove traces of Se compounds). The entire apparatus was placed in a fume-cupboard. Flows were allowed to stabilise at a given temperature for 30 mins before sampling and most experiments were conducted from low to high and from high to low temperature. The temperature programme of the GC oven was as follows: −30 °C for 2 min, then warming at 20 °C min^{-1} to 30 °C, then held for 2 min followed by heating at 20 °C min^{-1} to 150 °C and holding for 6 min. An HP-PONA (cross-linked methylsilicone gum) column (50 m, 0.2 mm internal diameter, film thickness 0.5 μm, phase ratio 100) was employed with helium as the carrier gas. Calibrations for 2-methylpropane and 2-methylpropene were carried out using standard gas mixtures‡ in connection with several gas sampling loop volumes (0.5–5 cm^3) and for group 16 compounds using

---

†Throughout this paper, the nomenclature d^n- is used to indicate that there are *n* deuterium atoms in the given compound. Thus, $\mathrm{d^{18}}$-$\mathrm{Bu^t_2Se}$ is $\mathrm{(C_4D_9)_2Se}$.

‡**CAUTION:** We have used three different samples of calibrant gas because, alarmingly, the first two gave different results. A sample nominally containing 1000 ppm (Scott Speciality Gases) each of 2-methylpropane and 2-methylpropene suggested that the MS detector is 1.6 times more sensitive to 2-methylpropene than to 2-methylpropane, whereas a sample nominally containing 100 ppm of each (Scott Speciality Gases) gave a sensitivity ratio of 1.05 : 1. In both cases, the response of the MS to both compounds was linear over the whole range. A third sample nominally containing 1000 ppm of each compound (Air Products) gave a ratio of 1 : 1.05 so we have assumed that the correct ratio is 1 : 1. In a previous paper,[29] which was submitted before we had carried out the third calibration, we assumed that the ratio of 1.6 : 1 was correct. The amounts quoted in that paper[29] are therefore wrong, but the interpretation of them is not greatly affected at least qualitatively.

published[34] or measured vapour pressure data. In cases where the total amount of hydrocarbon produced did not correlate exactly with the initial amount of precursor, it was assumed that the vapour pressure data for the precursor were in error (it is very sensitive to small changes in temperature) and the amount of precursor was adjusted to fit the amount of hydrocarbons produced.

Labelled compounds were measured quantitively using total ion currents (2-methylpropene) or single ion scans in the mass spectrum, as described previously.[27] Masses used were: 2-methylpropene, *m*/*z*: d^0 56 (M^+), d^8 64 (M^+); 2-methylpropane, *m*/*z*: d^0 43 ($[M-CH_3]^+$), d^1 44 ($[M-CH_3]^+$), d^2 45 ($[M-CH_3]^+$), d^9 49 ($[M-CD_3]^+$), d^{10} 50 ($[M-CD_3]^+$). These masses were chosen to avoid interferences. However, for d^0-2-methylpropane, there is an interference at *m*/*z* 43 from ($[M-CH_3-H]^+$) from d^1-2-methylpropane. This peak is 0.38 times the area of the peak at *m*/*z* 44 so the area of the peak at *m*/*z* 43 arising from d^1-2-methylpropane was calculated and subtracted from the total area of the peak to give the area arising solely from d^0-2-methylpropane. If d^2-2-methylpropane is present, the peak at *m*/*z* 44 has interferences from it ($[M-CH_2D]^+$ and ($[M-CH_3-H]^+$). We estimate that the ratio of the peak at *m*/*z* 45 : 44 in pure d^2-methylpropane should be 1.23 : 1. We can then use this to determine the $d^2 : d^1$ ratio. Values obtained using single ion scans were checked for consistency of the $(d^0+d^1+d^2) : (d^8+d^9+d^{10})$ ratio using total ion currents.

Baseline separations were obtained for all species apart from d^0-, d^1-, d^2-2-methylpropane and d^8-, d^9-, d^{10}-2-methylpropane. There was no evidence for d^n-2-methylpropene ($n \neq 0$ or 8) in any of the samples below 700 °C. At 700 °C extensive scrambling of H and D in the methyl groups of 2-methylpropene occurs, but this is also observed when 2-methylpropene is passed through a clean tube at 700 °C with D_2 as the carrier gas. Labelled methane was quantified as previously described.[27] Searches for H_2Se and $\mathrm{Bu^tSeH}$ were carried out using *m*/*z* 80 and 138, respectively.

Theoretical methods

Hartree–Fock and post Hartree–Fock *ab initio* molecular orbital techniques[35] and density functional theory (DFT) methods[36,37] have been used to study the proposed reaction mechanism from first principles. The C–Se bond dissociation energies for dialkyl selenides and alkylselenium radicals have been computed using the *ab initio* (ROHF and MP2) and density functional theory (DFT) methods (BHandH, BHandH-LYP, B3LYP, B3P86, B3PW91, BLYP and BP86) with the 6-311+G(2d,p) basis set.[38] All calculations were performed using the GAUSSIAN 94[39] implementation of the density functional theory (DFT) method while the SPARTAN 4.1.2[40] electronic structure program was used to generate starting structures and to animate vibrational frequencies. Geometry optimisation, critical point characterisation (all calculated structures were found to correspond to true energy minima), normal mode analysis (vibrational frequencies) and thermodynamic calculations[41–43] were carried out using the default GAUSSIAN convergence criteria.[44,45] All of the geometries for the molecules studied were fully optimised without using symmetry or structural constraints. A detailed analysis of the computed energies and comparison with experimental results along with an assessment of the suitability of the DFT methods, for the computational study of these systems, has been published by one of the authors recently.[38] Calculations were also performed using the SPARTAN 4.1.2 electronic structure program[39] and MOPAC93[46] programs. The PM3 (Parametric Method 3) method[47] a variant of the MNDO (modified neglect of differential overlap) method developed by Dewar *et al.*[48,49] was used. The standard semi-empirical program modules were used both for geometry optimisation, critical point characterisation (all calculated structures were found to correspond to true energy minima), normal mode analysis (vibrational frequencies) and thermodynamic calculations. Transition states were located using the linear synchronous transit (LST) technique.[50] In all cases a transition state was identified

Table 1 Gas-phase mechanism and reaction rate parameters[a]

Reaction	*A*	*m*	E_a	Ref.
$\mathrm{Bu^t{}_2Se \xrightarrow{3} Bu^tSe^\bullet + Bu^{t\bullet}}$	$10^{15.3}$	0	225.9	R
$\mathrm{Bu^tSe^\bullet \xrightarrow{4} Bu^{t\bullet} + Se}$	$10^{15.34}$	0	229.9	R
$\mathrm{2Bu^{t\bullet} \xrightarrow{5} C_4H_8{}^b + Bu^tH}$	$10^{16.53}$	−1.5	0	62
$\mathrm{2Bu^{t\bullet} \xrightarrow{6} Bu^t{}_2}$	$10^{16.1}$	−1.5	0	62
$\mathrm{Bu^{t\bullet} \xrightarrow{7} C_4H_8 + H^\bullet}$	$10^{9.34}$	1.48	150.6	63
$\mathrm{2H^\bullet + H_2 \xrightarrow{8a} 2H_2}$	$10^{18.74}$	−1.3	0	64
$\mathrm{2H^\bullet + He \xrightarrow{8b} H_2 + He}$	$10^{17.8}$	−1.0	0	64
$\mathrm{Bu^{t\bullet} + D_2 \xrightarrow{9} Bu^tD + D^\bullet}$	$10^{-2.37}$	4.43	45	R
$\mathrm{H^\bullet + H_2 \xrightarrow{10a} H_2 + H^\bullet}$	$10^{6.4}$	2.29	37.6	65
$\mathrm{H^\bullet + D_2 \xrightarrow{10b} HD + D^\bullet}$	$10^{7.01}$	2.1	29.3	66
$\mathrm{Bu^{t\bullet} + H^\bullet \xrightarrow{11a} Bu^tH}$	$10^{10.8}$	−0.15	0	62
$\mathrm{Bu^{t\bullet} + D^\bullet \xrightarrow{11b} Bu^tD}$	$10^{10.8}$	−0.15	0	R,62
$\mathrm{Bu^{t\bullet} + Bu^t{}_2Se \xrightarrow{12} Bu^tH + Bu^tSeC(CH_3)_2CH_2{}^\bullet}$	$10^{-5.3}$	5.2	37.9	R,60
$\mathrm{H^\bullet + Bu^t{}_2Se \xrightarrow{13} H_2 + Bu^tSeC(CH_3)_2CH_2{}^\bullet}$	$10^{5.8}$	2.4	10.8	R,60
$\mathrm{Bu^{t\bullet} + H_2 \xrightarrow{14} Bu^tH + H^\bullet}$	$10^{-1.7}$	4.24	37.5	62
$\mathrm{Bu^{t\bullet} + Bu^t{}_2Se \xrightarrow{15} Bu^tH + C_4H_8 + Bu^tSe^\bullet}$	N/C	N/C	N/C	R
$\mathrm{H^\bullet + Bu^t{}_2Se \xrightarrow{16} H_2 + C_4H_8 + Bu^tSe^\bullet}$	N/C	N/C	N/C	R
$\mathrm{Bu^t{}_2Se + Se \xrightarrow{18} Bu^t{}_2Se_2}$	N/C	N/C	N/C	R
$\mathrm{C_4H_8 + H_2 \xrightarrow{24'} Bu^tH}$	$10^{13.0}$	0	154.8	60
$\mathrm{Bu^tSeC(CH_3)_2CH_2{}^\bullet \xrightarrow{25} C_4H_8 + Bu^tSe^\bullet}$	$10^{13.7}$	0	133.9	R,60
$\mathrm{C_4H_8 + H^\bullet \xrightarrow{26} Bu^{t\bullet}}$	$10^{12.79}$	0.25	6.1	63
$\mathrm{Bu^{t\bullet} + H^\bullet \xrightarrow{27} C_4H_8 + H_2}$	$10^{12.7}$	0	0	62
$\mathrm{Bu^tH + H^\bullet \xrightarrow{28} Bu^{t\bullet} + H_2}$	$10^{5.8}$	2.4	10.8	62

[a] Rate data for hydrocarbon and deuterated species were obtained from the literature.[62–66] The kinetic rate constant is of the form $k = AT^m \exp(-E_a/RT)$.[60] The units of E_a and *A* are (kJ mol^{-1}) and $(mol\ cm^{-3})^{1-n}\ s^{-1}$ respectively, where *n* is the order of reaction. Concentrations are in mol cm^{-3} and time in s. All rate data for Se-centred species were obtained from DFT and canonical transition state theory (CTST) as explained in the text. R indicates data estimated in this work. R,60 indicates data combined from R and ref. 60. N/C indicates not calculated. [b] C_4H_8 = 2-methylpropene.

Table 2 Gas-phase mechanism and reaction rate parameters for reactions not thought to be of significance in the thermal decomposition of $Bu^t{}_2Se$[a]

Reaction	A	n	E_a	Ref.
$Bu^t{}_2Se \xrightarrow{29} Bu^tSeH + C_4H_8$[b]	$10^{13.5}$	0	234.3	R
$Bu^tSeH \xrightarrow{30} C_4H_8 + H_2Se$	$10^{13.3}$	0	242.7	R
$Bu^tSeH \xrightarrow{31} Bu^tH + Se$	$10^{13.3}$	0	225.9	R
$Bu^t{}_2 \xrightarrow{32} 2Bu^{t\bullet}$	$10^{17.1}$	0	292.9	60
$Bu^{t\bullet} + C_4H_8 \xrightarrow{33} Bu^tH + CH_2C(Me)CH_2{}^\bullet$	$10^{11.3}$	0	41.8	60
$CH_2C(Me)CH_2{}^\bullet + Bu^t{}_2Se \xrightarrow{34} C_4H_8 + Bu^tSeC(CH_3)_2CH_2{}^\bullet$	$10^{12.40}$	0	85.8	60
$CH_2C(Me)CH_2{}^\bullet + H^\bullet \xrightarrow{35} C_4H_8$	$10^{13.7}$	0	0	60
$CH_2C(Me)CH_2{}^\bullet + CH_2C(Me)CH_2{}^\bullet \xrightarrow{36} C_8H_{14}$	$10^{13.30}$	−1.5	0	60
$Bu^{t\bullet} + CH_2C(Me)CH_2{}^\bullet \xrightarrow{37} Bu^tCH_2C(Me)CH_2$	$10^{15.0}$	−0.75	0	60
$Bu^t{}_2Se \xrightarrow{38} Bu^t{}_2 + Se$	$10^{11.3}$	0	581.6	R

[a]Calculations and units are as in Table 1. Rate data for allyl hydrocarbon species were obtained from the literature.[60] [b]C_4H_8 = 2-methylpropene.

when the Hessian yielded only one significant imaginary frequency ($400i\ cm^{-1} \leqslant \nu_{TS} \leqslant 2000i\ cm^{-1}$). Verification that the coordinate corresponding to the imaginary frequency smoothly connects reactants and products was undertaken by 'animating' the coordinate whilst in ambiguous cases the intrinsic reaction co-ordinate (IRC) method implemented in MOPAC 93[46] was used. In all computations the default convergence criteria were used.

Rate constants for all reactions involving Se-centred species were estimated using canonical transition state theory (CTST). The CTST calculations are based solely on the statistical thermodynamic properties of the reactants and the transition state. Enthalpies of activation, moments of inertia, and vibrational frequencies obtained from quantum chemical computations were used to compute the partition functions of the reactants and the transition state. No corrections for quantum mechanical tunnelling were made from CTST since such corrections would be expected to be small for MOVPE reactions since relatively high temperatures and large molecules are involved. The computed values of the rate parameters are collected in Tables 1 and 2.

Rather than deduce the specific contributions of individual reactions directly from experimental data, a procedure not yet possible given the current state of knowledge, we chose to define all the reactions that are expected to occur, assigned numerical values to the appropriate rate parameters and numerically solved the resultant differential equations, comparing the numerical solutions with experimental data as a test of the validity of the chosen reaction set.

The purpose of the present study was to perform a thorough numerical simulation of $Bu^t{}_2Se$ pyrolysis using comprehensive reaction schemes with rate parameters evaluated from the computational quantum chemistry calculations. It was not initially our intention to establish the definitive 'correct' mechanism for the pyrolysis processes. This will obviously be limited by the present status of knowledge of organoselenium free-radical chemistry and the appropriateness of the chosen theoretical model (*e.g.* accuracy and precision of rate parameters, types of reactions which occur, validity of hydrocarbon experimental data). The present study was used in determining specific reactions which may warrant closer study and in planning specific pyrolysis experiments to test certain features of the proposed mechanism. It should be emphasised that these computations do not involve parameter fitting and are therefore independent of the experiment that is being modelled. In establishing the matrix of chemical reactions upon which the simulations were based, the approach adopted was to include all conceivable species and processes. Comparison of the simulated data with the experimental results readily indicated which of the reactions were superfluous.

The decomposition experiment was approximated as an isothermal constant-volume pyrolysis and is described by a system of differential equations constructed by the rigorous application of mass-action principles. This system contains an equation for each chemical species in the model, and each equation expresses the time derivative of this species in terms of the usual mass-action products. With numerical values assigned to all the rate constants, and a starting pressure/concentration selected for the precursor, this becomes an initial value problem in the solution of non-linear ordinary differential equations (ODEs). Numerical solution of these so called 'stiff systems' was accomplished using the built in solver for stiff ODE systems using the semi-implicit extrapolation modification of the Burlisch–Stoer method in Mathcad 6.0.[51,52]

Since the diffusion velocities of the gas species can be estimated to be an order of magnitude less than the average flow velocity, the conditions in the flow tube were simulated by specifying initial non-zero partial pressures for only the $Bu^t{}_2Se$ and the He/H_2 (D_2) carrier gas. The diffusion times of H and D radicals to the walls of the furnace tube were estimated to be 0.2 s based on an estimated diffusion coefficient of $2\ cm^2\ s^{-1}$ and a furnace tube radius of 3 cm. Errors in the isothermal assumption on which the simulations were performed are significant at temperatures above 500 °C, because at higher temperatures the reactions occur in the steep thermal gradients at the inlet to the furnace.

Results

Thermal decomposition of $Bu^t{}_2Se$

Heating $Bu^t{}_2Se$ in helium produces 2-methylpropene and 2-methylpropane in an 8 : 1 ratio [Fig. 3(a)]. Very careful analysis of the GCMS traces using total ion currents or suitable single ion scans shows that neither Bu^tSeH nor H_2Se is detectable as a product at any temperature, although we have shown in separate experiments that both Bu^tSeH (50% decomposition at 350 °C) and H_2Se (stable over the whole temperature range) are sufficiently stable under the reaction conditions that they would be detectable if they were formed.[53]

Carrying out the same reaction in a hydrogen ambient produces almost identical results with a slight decrease in decomposition temperature and a ratio of 2-methylpropene : 2-methylpropane of 8 : 1 [Fig. 3(b)]. The 2-methylpropene : 2-methylpropane ratios at different extents of decomposition are also almost identical in hydrogen or helium (Fig. 4). If the decomposition is carried out in D_2, the 2-methylpropane formed contains some D; $(CH_3)_3CH : (CH_3)_3CD = 10$.

Decomposition of d^{18}-$Bu^t{}_2Se$

In helium, the decomposition of d^{18}-$Bu^t{}_2Se$ produces the d^8-2-methylpropene and d^{10}-2-methylpropane. In hydrogen, both 2-methylpropene and 2-methylpropane are formed, but in this case, there is substantial incorporation of H into the 2-

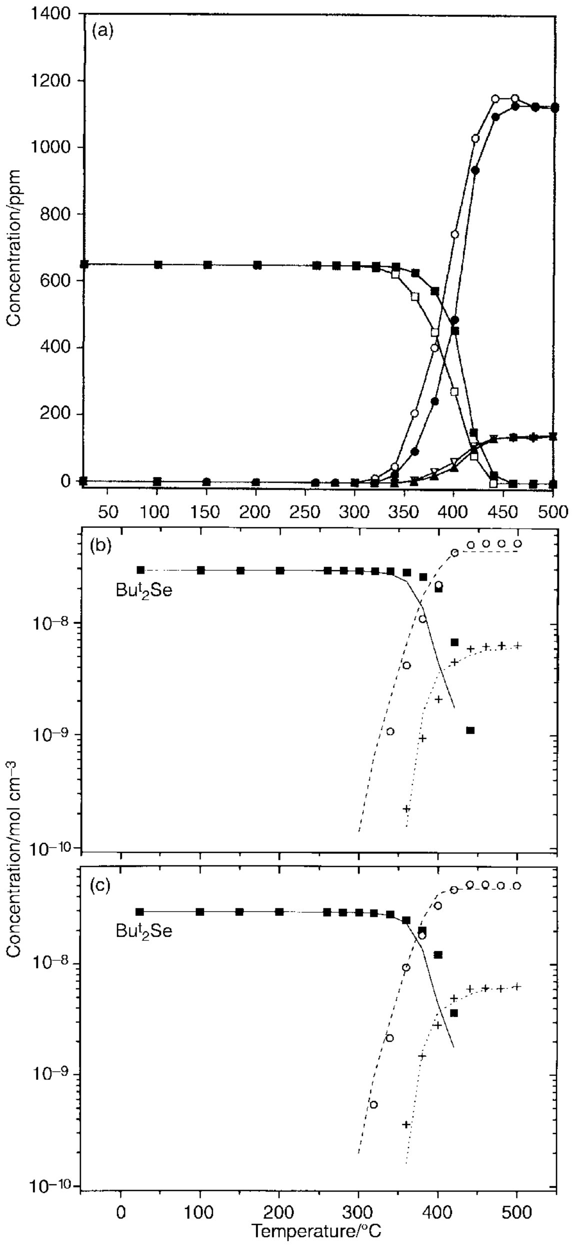

Fig. 3 Reaction profiles for the decomposition of Bu$^t_2$Se. (a) In helium (■) Bu$^t_2$Se, (●) 2-methylpropene, (▲) 2-methylpropane or hydrogen (□) Bu$^t_2$Se, (○) 2-methylpropene, (▽) 2-methylpropane. (b) In helium (■) Bu$^t_2$Se, (○) 2-methylpropene, (✚) 2-methylpropane. (c) In hydrogen (■) Bu$^t_2$Se, (○) 2-methylpropene, (✚) 2-methylpropane. Lines in (b) and (c) are values calculated from the theoretical simulations based on the reactions of Scheme 4 and the parameters of Table 1.

methylpropane [$(CD_3)_3CH : (CD_3)_3CD = 2.6 : 1$ at 50% decomposition, falling to 1.4 : 1 at full decomposition].§

Codecomposition of d^0 and d^{18}-Bu$^t_2$Se

The codecomposition of d^0- and d^{18}- Bu$^t_2$Se (1.2 : 1) in helium produces only 2-methylpropene (d^0 : d^8 = 1.4 : 1) and 2-methylpropane (d^0 : d^1 : d^9 : d^{10} = 2.29 : 1 : 2.86 : 1.2). There is no evidence for formation of any d^9-Bu$^t_2$Se at any of the temperatures we have studied.

Codecomposition of Bu$^t_2$Se and Me$_2$Zn

The codecomposition of Bu$^t_2$Se and Me$_2$Zn in helium produces methane and 2-methylpropene as the major products, whilst

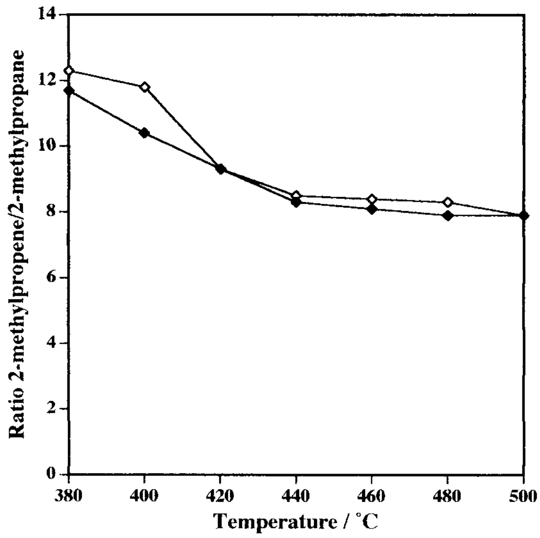

Fig. 4 Ratio of 2-methylpropene : 2-methylpropane at different temperatures during the decomposition of Bu$^t_2$Se in helium (♦) or hydrogen (◊).

using d^{18}-Bu$^t_2$Se in this reaction gives mainly CH_3D, ($CH_3D : CH_4 = 3.4 : 1$) and d^8-2-methylpropene. Small amounts of CH_4 are present even at room temperature, presumably from reaction of Me$_2$Zn with moisture.

Carrying out the codecomposition of Me$_2$Zn and d^{18}-Bu$^t_2$Se in hydrogen does generate some 2-methylpropane (mainly d^8) in addition to the other products (the methane is mainly CH_4 ($CH_4 : CH_3D = 3.3 : 1$); d^2-2-methylpropane is formed from the reaction of Me$_2$Zn with d^0-Bu$^t_2$Se in D_2. The amount of 2-methylpropane formed increases at higher temperatures and after complete loss of Bu$^t_2$Se.

Photochemical decomposition of Bu$^t_2$Se

UV photolysis of Bu$^t_2$Se in helium at room temperature causes *ca.* 29% decomposition under our conditions and produces equal amounts of 2-methylpropene and 2-methylpropane, together with small amounts of 2,2,3,3-tetramethylbutane and some Bu$^t_2$Se$_2$. Co-photolysing d^0- and d^{18}-Bu$^t_2$Se (1 : 3 ratio) produces d^0- and d^8-2-methylpropene together with d^0-, d^1-, d^9- and d^{10}- 2-methylpropane (1 : 1.6 : 3.5 : 4.8). d^9-Bu$^t_2$Se is produced (final d^0 : d^9 : d^{18}ratio is 6.6 : 1 : 14.7) together with d^0- and d^{18}-Bu$^t_2$Se$_2$. There is no sign of d^9-Bu$^t_2$Se$_2$.

Discussion

Decomposition of Bu$^t_2$Se

Thermal. The possible initial steps in the decomposition of Bu$^t_2$Se, reductive elimination, β-hydrogen abstraction and homolytic cleavage are shown in Fig. 5. Since 2,2,3,3-tetramethylbutane is not observed as a product, reductive elimination can be ruled out as the first step of the reaction. The fact that neither Bu^{t}SeH nor H_2Se is observed as products under conditions where they would both be expected to be stable rules out β-H abstraction as a possible decomposition pathway for Bu$^t_2$Se and suggests that the initial step in the decomposition must be Se–C bond cleavage to give Bu$^{t\cdot}$ and Bu^{t}Se$^\cdot$ [eqn. (3), Scheme 2].

In order to distinguish unequivocally between β-hydrogen abstraction and free radical pathways, we have carried out the co-decomposition of d^0 and d^{18}-Bu$^t_2$Se (1.2 : 1). In principle, since β-hydrogen abstraction to give Bu^{t}SeH followed by β-hydrogen abstraction/reductive elimination is all intramolecular, the 2-methylpropane produced should be all d^0 or d^{10} whilst a free radical process will lead to a mixture of d^0, d^1, d^9 and d^{10} since the free Bu$^{t\cdot}$ can abstract H from species derived

---

§ H_2Se is observed as an impurity in the initial precursor, but its concentration does not alter with the extent of decomposition.

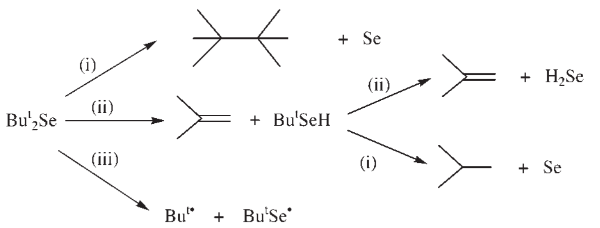

Fig. 5 Possible first steps in the decomposition of Bu^t_2Se. (i) reductive elimination; (ii) β-H abstraction; (iii) homolytic fission of the Se–C bond to give free radicals.

$$Bu^t_2Se \longrightarrow Bu^tSe^{\cdot} + Bu^{t\cdot} \qquad (3)$$

$$Bu^tSe^{\cdot} \longrightarrow Bu^{t\cdot} + Se \qquad (4)$$

$$2\,Bu^{t\cdot} \longrightarrow C_4H_8 + C_4H_{10} \qquad (5)$$

$$2\,Bu^{t\cdot} \longrightarrow C_8H_{18} \qquad (6)$$

$$Bu^{t\cdot} \longrightarrow C_4H_8 + H^{\cdot} \qquad (7)$$

$$2\,H^{\cdot} \xrightarrow{\text{third body}} H_2 \qquad (8)$$

$$Bu^{t\cdot} + D_2 \longrightarrow C_4H_9D + D^{\cdot} \qquad (9)$$

$$H^{\cdot} + D_2 \longrightarrow HD + D^{\cdot} \qquad (10)$$

$$Bu^{t\cdot} + D^{\cdot} \longrightarrow C_4H_9D \qquad (11)$$

Scheme 2 Reactions involved in the decomposition of Bu^t_2Se if the only reactions of $Bu^{t\cdot}$ are simple gas phase reactions with itself or with the carrier gas (D_2).

either from d^0- or d^{18}-Bu^t_2Se. In practice, we observe d^0, d^1, d^9 and d^{10}-2-methylpropane in the ratio 2.29 : 1 : 2.86 : 1.2, suggesting that a free radical process is operating with kinetic isotope effects favouring H abstraction. However, this is not unequivocal proof because we have shown that the H directly attached to Se is readily exchanged[53] so that C_4D_9SeD and C_4H_9SeH will exchange to give a mixture of the starting species together with the exchange species, C_4H_9SeD and C_4D_9SeH, so that 2-methylpropane formed from them would also be d^0, d^1, d^9 and d^{10}. However, if we assume that β-hydrogen abstraction followed by reductive elimination [step (ii) followed by step (i) in Fig. 5] is responsible for the formation of 2-methylpropane, we can assume that β–H abstraction gives d^0- and d^{10}-Bu^tSeH in the ratio 0.8 : 1 (the same ratio as $C_4H_9X : C_4D_9X$, X = H or D in the final product). If the SeH/D equilibrium is then fully established and is followed by reductive elimination, the ratio of $d^0 : d^1 : d^9 : d^{10}$-2-methylpropane would be 1 : 1.25 : 1.25 : 1.56, far from the observed 2.29 : 1 : 2.86 : 1.2. However a free radical process in which there is a kinetic isotope effect (k_H/k_D) of *ca.* 2.3 fully accounts for the observed ratios. The increased amounts of products derived from d^9-$Bu^{t\cdot}$ relative to those from d^0-$Bu^{t\cdot}$ arise because more of the d^0-Bu^t_2Se is consumed by $H^{\cdot}$ abstraction (see later) so more d^{18}-Bu^t_2Se is available towards the end of the reaction for the generation of d^9-$Bu^{t\cdot}$.

The fact that d^9-Bu^t_2Se is produced on photolysis of a mixture of d^0- and d^{18}-Bu^t_2Se at room temperature but not on thermolysis of the same mixture indicates that recombination of $Bu^tSe^{\cdot}$ with $Bu^{t\cdot}$ does not occur to a significant extent in the high temperature reactions. This must either be because $Bu^tSe^{\cdot}$ is unstable, or because it reacts faster with other species than with $Bu^{t\cdot}$. The only other reactions available to it in helium would be with Bu^t_2Se, presumably this would be by H abstraction, but since the expected product (Bu^tSeH) is not observed, we conclude that $Bu^tSe^{\cdot}$ decomposes rapidly once it forms. This decomposition must be either *via* Se–C bond cleavage [eqn. (4), Scheme 2], or by loss of $H^{\cdot}$ to give 2-methylpropene and Se, although calculations (see later) show that this last reaction is thermodynamically inaccessible because two high energy species, $H^{\cdot}$ and $Se_{(g)}$ would be formed. The only other alternative would be by β-H abstraction to give $HSe^{\cdot}$, which would be expected to give a route to H_2Se (not observed). Bu^t_2Se then decomposes by cleavage of the two Se–C bonds to give $2 \times Bu^{t\cdot}$ and Se. However, this does not explain the products, 2-methylpropane and 2-methylpropene, nor their ratio.

It would be possible to explain the observed products and their ratio on the basis of simple reactions of $Bu^{t\cdot}$ with one another. At low temperatures, $Bu^{t\cdot}$ react together by disproportionation and combination to give 2-methylpropane and 2-methylpropene (1 : 1) together with 2,2,3,3-tetramethylbutane (10%, invariant with temperature).[54] However, above 380 °C, in the temperature region of our studies, the unimolecular loss of $H^{\cdot}$ from $Bu^{t\cdot}$ becomes competitive and dominates at higher temperatures. The disproportionation and combination reactions have zero activation energy, whereas the loss of $H^{\cdot}$ has a marked temperature dependence. This means that, at above 400 °C, the loss of $H^{\cdot}$ completely dominates and 2-methylpropene is the only product arising solely from $Bu^{t\cdot}$, particularly as recombination of $Bu^{t\cdot}$ with $H^{\cdot}$ is non-competitive with other reactions of $H^{\cdot}$.[54] Simple reactions of $Bu^{t\cdot}$ with one another, as shown in Scheme 2 can then be ruled out as being the sole mechanism by which reactions subsequent to Se–C bond cleavage occur.

For Pr^i_2Te, Hicks has proposed[55] a similar mechanism (shown in Fig. 6) to that described in Scheme 2, except that it involves surface bound free radicals which undergo β-H abstraction to give propene and surface bound $H^{\cdot}$. Propane is then formed by combination of $Pr^{i\cdot}{}_{(ads)}$ with $H^{\cdot}{}_{(ads)}$ (Fig. 6). For Bu^t_2Se, a similar process would give 2-methylpropene, 2-methylpropane and $H^{\cdot}{}_{(ads)}$ (Scheme 2). The relative rates of $H^{\cdot}$ abstraction, $H^{\cdot}{}_{(ads)}$ addition to $Bu^{t\cdot}{}_{(ads)}$ and combination of two $H^{\cdot}{}_{(ads)}$ [eqns. (7), (11) and (8), Scheme 2] then determine the ratio of 2-methylpropene : 2-methylpropane and a value of 8 : 1 is possible with the residual $H^{\cdot}{}_{(ads)}$ combining on the surface to give H_2. It is possible, invoking this mechanism, to explain the observation that in H_2 the ratio of 2-methylpropane : 2-methylpropene is unchanged relative to the value in helium but also that the labelling studies clearly show that H/D from the ambient H_2/D_2 is incorporated to a very significant extent (up to 70%). If incorporation occurred by direct reaction of $Bu^{t\cdot}{}_{(ads)}$ with D_2 or d^8-$Bu^{t\cdot}{}_{(ads)}$ with H_2 [eqn. (9), Scheme 2],

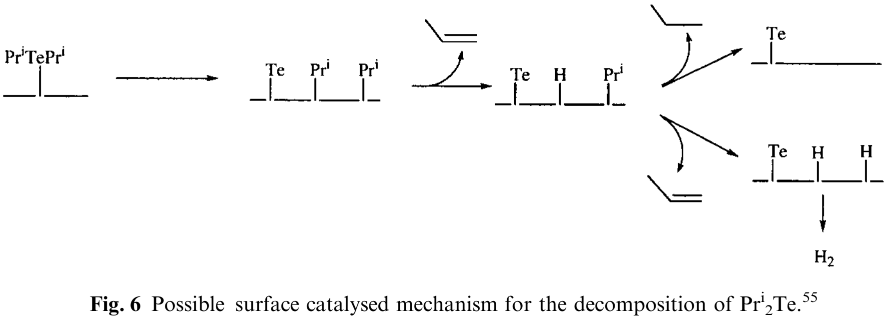

Fig. 6 Possible surface catalysed mechanism for the decomposition of Pr^i_2Te.[55]

the relative amount of 2-methylpropane would increase dramatically. However, the reactions shown in Scheme 2, eqns. (7)–(11) occurring on the surface would adequately account for the ratio of 2-methylpropene : 2-methylpropane being the same in He as in H_2 but also for the incorporation of H from the carrier gas into 2-methylpropane. These reactions require that Bu$^{t\cdot}_{(ads)}$ does not react with D_2, but that H$^{\cdot}_{(ads)}$ does to give HD and D$^{\cdot}_{(ads)}$. The 2-methylpropane is formed by recombination of Bu$^{t\cdot}_{(ads)}$ with H$^{\cdot}_{(ads)}$. In this scheme, the concentration of H$^{\cdot}_{(ads)}$ is not altered by changing from He to H_2 as ambient, only its labelling pattern so that, ignoring isotope effects, the ratio of 2-methylpropane : 2-methylpropene should be the same, but there is a pathway for incorporating H/D from the ambient H_2/D_2. This mechanism requires that the rate of reaction of H$^{\cdot}_{(ads)}$ with D_2 is very much faster than the rate of reaction of Bu$^{t\cdot}_{(ads)}$ with D_2. We have calculated the rate constants at various different temperatures (Table 3) and find that the rate constant for abstraction of D from D_2 by Bu$^{t\cdot}$ is lower than that for abstraction by H$^{\cdot}$ by a factor of 1000 or more over the entire temperature range investigated here.

We cannot unequivocally rule out the reactions of Scheme 2, occurring on the surface, as being wholly responsible for the decomposition of Bu$^t_2$Se, but other workers have suggested that glass surfaces do not strongly absorb Bu$^t_2$Se[26] and related alkyls[55] and that gas-phase reactions dominate when glass is the only exposed surface.[26] In our reactions, Se sublimes from the tube at all temperatures where decomposition of Bu$^t_2$Se is occurring and the glass always appears clean at the start and finish of the reaction, confirming that the precursors are not exposed to surfaces other than glass and that surface catalysed processes are probably not important. We therefore think it unlikely that surface processes occur in the decomposition of Bu$^t_2$Se.

Table 3 Calculated rate constants, k, for the gas-phase reactions of H_2 with Bu$^{t\cdot}$ or of H_2 with H$^{\cdot a}$

T/°C	k/cm^3 mol^{-1} s^{-1} H$^{\cdot}$ with H_2 (k_H)	Bu$^{t\cdot}$ with H_2(k_B)	k_H/k_B
300	1.3×10^{10}	3.4×10^{6}	3.9×10^{3}
320	1.8×10^{10}	5.1×10^{6}	3.5×10^{3}
340	2.3×10^{10}	7.6×10^{6}	3.0×10^{3}
360	3.0×10^{10}	1.1×10^{7}	2.7×10^{3}
380	3.7×10^{10}	1.6×10^{7}	2.4×10^{3}
400	4.7×10^{10}	2.2×10^{7}	2.2×10^{3}
420	5.8×10^{10}	3.0×10^{7}	1.9×10^{3}
440	7.1×10^{10}	4.0×10^{7}	1.8×10^{3}
460	8.6×10^{10}	5.4×10^{7}	1.6×10^{3}
480	1.0×10^{11}	7.1×10^{7}	1.5×10^{3}
500	1.2×10^{11}	9.3×10^{7}	1.3×10^{3}

[a] Calculated using the equation $k = AT^m\exp(-E_A/RT)$; for H$^{\bullet}$, $A = 1\times10^7$ cm^3 mol^{-1} s^{-1}, $m = 2.1$, $E_A = 29.3$ kJ mol^{-1}; for Bu$^{t\bullet}$, $A = 0.0185$ cm^3 mol^{-1} s^{-1}, $m = 4.24$, $E_A = 37.8$ kJ mol^{-1}.

$$\mathrm{Bu^t_2Se} \longrightarrow \mathrm{Bu^tSe^{\bullet}} + \mathrm{Bu^{t\bullet}} \tag{3}$$

$$\mathrm{Bu^tSe^{\bullet}} \longrightarrow \mathrm{Bu^{t\bullet}} + \mathrm{Se} \tag{4}$$

$$\mathrm{Bu^{t\bullet}} + \mathrm{Bu^t_2Se} \longrightarrow \mathrm{C_4H_{10}} + 2\,\mathrm{C_4H_8} + \mathrm{Se} + \mathrm{H^{\bullet}} \tag{12}$$

$$\mathrm{H^{\bullet}} + \mathrm{Bu^t_2Se} \longrightarrow \mathrm{H_2} + 2\,\mathrm{C_4H_8} + \mathrm{Se} + \mathrm{H^{\bullet}} \tag{13}$$

$$\mathrm{Bu^{t\bullet}} + \mathrm{H_2} \longrightarrow \mathrm{C_4H_{10}} + \mathrm{H^{\bullet}} \tag{14}$$

$$2\,\mathrm{H^{\bullet}} \xrightarrow{\text{third body}} \mathrm{H_2} \tag{8}$$

$$\mathrm{Bu^{t\bullet}} \longrightarrow \mathrm{C_4H_8} + \mathrm{H^{\bullet}} \tag{7}$$

$$2\,\mathrm{Bu^{t\bullet}} \longrightarrow \mathrm{C_4H_8} + \mathrm{C_4H_{10}} \tag{5}$$

$$\mathrm{Bu^{t\bullet}} + \mathrm{H^{\bullet}} \longrightarrow \mathrm{C_4H_{10}} \tag{17}$$

Scheme 3 Reactions involved in the decomposition of Bu$^t_2$Se assuming a concerted reaction of Bu$^{t\cdot}$ or H$^{\cdot}$ with intact Bu$^t_2$Se [eqns. (12) and (13)].

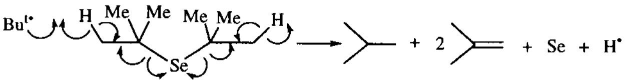

Fig. 7 Concerted mechanism for the reaction of Bu$^{\bullet}$ with Bu$^t_2$Se [eqn. (12) of Scheme 3].

The only alternative fate for Bu$^{t\cdot}$ is that it will react with intact Bu$^t_2$Se, which, at least in helium, will be the major reactive species present. It cannot react by addition, since this would provide a pathway to d^9-Bu$^t_2$Se, which is not observed on codecomposition of d^0- and d^{18}-Bu$^t_2$Se; so it must react by abstracting a β-H atom. There are two possible pathways that can occur subsequent to H abstraction. One is shown in eqn. (12), Scheme 3 and Fig. 7 and is analogous to the process that we have already proposed on the basis of labelling studies for the reaction of Pr$^{i\cdot}$ with Pr$^i_2$Te.[27] Abstraction of H$^{\cdot}$ from Bu$^t_2$Se by Bu$^{t\cdot}$ leads to 2-methylpropane, 2 × 2-methylpropene, Se and H$^{\cdot}$. H$^{\cdot}$ then reacts with intact Bu$^t_2$Se in a similar manner to give H_2, 2 × 2-methylpropene, Se and regenerate H$^{\cdot}$ [eqn. (13), Scheme 3]. This is then a chain propagation reaction with termination occurring by reaction of H$^{\cdot}$ with H$^{\cdot}$ (needs a third body to remove excess energy) or with Bu$^{t\cdot}$ to give Bu^{t}H [eqn. (8) or (17) Scheme 3]. An 8 : 1 ratio of 2-methylpropene : 2-methylpropane is then easily achieved since the chain propagating reaction only produces 2-methylpropene whilst the 2-methylpropane is formed in the initiation and termination steps. We have drawn the decomposition of Bu^{t}SeC$_4$H$_8{}^{\cdot}$, formed after abstraction of H$^{\cdot}$ from Bu$^t_2$Se by Bu$^{t\cdot}$ or H$^{\cdot}$, as a concerted reaction in the gas phase. Calculations (see below) suggest that this concerted reaction is very unlikely since it produces two highly energetic species, H$^{\cdot}$ and Se$_{(g)}$. The reaction could occur on a surface, to produce Se$_{(s)}$ and H$_{(ads)}$, both of which are of much lower energy than the gas phase species, or it could occur stepwise in the gas phase with H$^{\cdot}$ being lost from Bu$^{t\cdot}$, a reaction which is known to occur in this temperature regime[54] (see above). The decomposition mechanism is then as shown in Scheme 4, omitting eqn. (14).

In hydrogen, it is expected that Bu$^{t\cdot}$ will react with H_2 to give 2-methylpropane and H$^{\cdot}$ [eqn. (14), Scheme 4]. Whether the chain reaction is initiated directly by Bu$^{t\cdot}$ [eqn. (15), Scheme 4] or by Bu$^{t\cdot}$ reacting with H_2 to give H$^{\cdot}$ [eqns. (14) and (16), Scheme 4], the ratio of 2-methylpropene : methylpropane should be identical, thus accounting for the similarity of observations in helium and hydrogen ambient. Eqn. (14), Scheme 4, however provides a mechanism for the incorpora-

Initiation

$$\mathrm{Bu^t_2Se} \longrightarrow \mathrm{Bu^tSe^{\bullet}} + \mathrm{Bu^{t\bullet}} \tag{3}$$

Propagation

$$\mathrm{Bu^tSe^{\bullet}} \longrightarrow \mathrm{Bu^{t\bullet}} + \mathrm{Se} \tag{4}$$

$$\mathrm{Bu^{t\bullet}} + \mathrm{Bu^t_2Se} \longrightarrow \mathrm{C_4H_{10}} + \mathrm{C_4H_8} + \mathrm{Bu^tSe^{\bullet}} \tag{15}$$

$$\mathrm{Bu^{t\bullet}} \longrightarrow \mathrm{C_4H_8} + \mathrm{H^{\bullet}} \tag{7}$$

$$\mathrm{H^{\bullet}} + \mathrm{Bu^t_2Se} \longrightarrow \mathrm{H_2} + \mathrm{C_4H_8} + \mathrm{Bu^tSe^{\bullet}} \tag{16}$$

$$\mathrm{Bu^{t\bullet}} + \mathrm{H_2} \longrightarrow \mathrm{C_4H_{10}} + \mathrm{H^{\bullet}} \tag{14}$$

Termination

$$2\,\mathrm{H^{\bullet}} \xrightarrow{\text{third body}} \mathrm{H_2} \tag{8}$$

$$2\,\mathrm{Bu^{t\bullet}} \longrightarrow \mathrm{C_4H_8} + \mathrm{C_4H_{10}} \tag{5}$$

$$\mathrm{Bu^{t\bullet}} + \mathrm{H^{\bullet}} \longrightarrow \mathrm{C_4H_{10}} \tag{17}$$

Scheme 4 Proposed mechanism for the decomposition of Bu$^t_2$Se in hydrogen or helium.

tion of $\mathrm{H_2/D_2}$ from the ambient into the product 2-methylpropane.

Scheme 4 provides a mechanism for the decomposition of $\mathrm{Bu^t{}_2Se}$ that is consistent with all of the experimental observations that we have made. It also explains the larger amounts of d^0- and d^9-2-methylpropane (than of d^1- and d^{10}) obtained on codecomposition of d^0- and d^{18}-$\mathrm{Bu^tSe}$ in helium since there is likely to be a significant isotope effect operating on the $\mathrm{H^{\cdot}}$ abstraction reactions, eqns. (15) and (16), Scheme 4. This isotope effect also accounts for the larger amounts of d^0-2-methylpropene produced.

Other possible reactions, which may become competitive at high percentage decomposition of $\mathrm{Bu^t{}_2Se}$, include the abstraction of H from 2-methylpropene or 2-methylpropane by $\mathrm{Bu^{t\cdot}}$ or $\mathrm{H^{\cdot}}$. For 2-methylpropane, H abstraction would occur from the tertiary C atom to give $\mathrm{Bu^{t\cdot}}$, thus proceeding back into the cycle and not altering the ratio of 2-methylpropene to 2-methylpropane. However, the low concentration of 2-methylpropane except at high conversion makes this sequence unlikely. For 2-methylpropene, a methyl H atom would be abstracted to give the (allyl) stabilised 2-methylpropenyl radical. This reaction would be thermodynamically favourable but would lead to 2,5-dimethylhexa-1,5-diene from coupling[56] or to scrambling of the H/D labels in the methyl groups of the 2-methylpropene formed from codecomposition of d^0- and d^{18}-$\mathrm{Bu^t{}_2Se}$. No such scrambling is observed, nor is 2,5-dimethylhexa-1,5-diene, so H abstraction from 2-methylpropene cannot be occurring. Our calculations (see below) confirm that, despite being thermodynamically favourable, H abstraction from 2-methylpropene is not a competitive reaction.

Calculations. In order to try to substantiate the mechanism that we are proposing for the decomposition of $\mathrm{Bu^t{}_2Se}$, we have carried out *ab initio* and density functional theory (DFT) calculations on all of the Se-centred reactions shown in Tables 1 and 2. Our new calculations show that the activation parameters for a β-hydrogen abstraction within $\mathrm{Bu^t{}_2Se}$ are such that this process can be ignored as a possible decomposition pathway, and that the lowest energy first step is homolytic fission of the Se–C bond. This conclusion contradicts our earlier deductions[26] concerning the activation energies for the β-hydride elimination reactions computed using the PM3 method. This discrepancy is discussed elsewhere.[57] The conclusion is, however in agreement with those of Benson, who has suggested that current kinetic interpretations of the pyrolysis of alkyl sulfides, disulfides and mercaptans are all seriously in error.[58] The most serious errors have to do with the presumed four-centre β-hydride elimination reaction[59,60] of either $\mathrm{H_2S}$ from RSH or RSH from $\mathrm{R_2S}$. He suggests that this reaction may be too slow to be important in pyrolysis and this indeed has been found from both DFT and MP2 calculations for both sulfur and selenium centred alkyls and alkyl hydrides,[38] *viz.* the activation energies for the β-hydride elimination reactions forming $\mathrm{H_2Se}$ from $\mathrm{Bu^tSeH}$ or $\mathrm{Bu^tSeH}$ from $\mathrm{Bu^t{}_2Se}$ are $\geqslant 230\ \mathrm{kJ\ mol^{-1}}$ and of no importance under standard growth and pyrolysis conditions (300–500 °C). A different situation appears to exist with the experimental data on As compounds.[61]

The free radical mechanism proposed to account for the pyrolysis of $\mathrm{Bu^t{}_2Se}$ in both dihydrogen and helium is listed along with the relevant kinetic data in Tables 1 and 2. Alkyl radical gas phase chemistry is well documented and the kinetic parameters for these steps were obtained from the combustion literature.[62,63] Rate constants for the reversible loss of hydrogen from $\mathrm{Bu^{t\cdot}}$ were taken from the paper of Gutman and co-workers.[63] The recombination of two $\mathrm{H^{\cdot}}$ was taken from Tsang and Hampson,[64] while reactions involving hydrogen and deuterium and their radicals were taken from the papers of Michael *et al.*[65,66]

However, a problem arises because one reaction rate constant with one set of Arrhenius parameters is unable to describe the temperature dependence of reactions as complex as (15) and (16). Intuitively one can see this by examining the concerted reactions in more detail. Such reactions are not microscopically reversible, since it is extremely unlikely that two isobutene molecules and one isobutane/dihydrogen molecule could simultaneously collide with a selenium atom and hydrogen atom to regenerate a molecule of $\mathrm{Bu^t{}_2Se}$.[67] [The enthalpy change for the concerted reactions is prohibitively endothermic ($>400\ \mathrm{kJ\ mol^{-1}}$), principally as a result of the production of hydrogen radicals and gaseous Se. Just as important however is the unfavourable A factor. The entropy change for three molecules (two molecules of isobutene and one isobutane/dihydrogen molecule) forming a single transition state can be estimated[60] at *ca.* $-251\ \mathrm{J\ mol^{-1}\ K^{-1}}$. At a standard state of $1\ \mathrm{mol\ dm^{-3}}$, this would become $-197\ \mathrm{J\ mol^{-1}\ K^{-1}}$, yielding an A factor of *ca.* $10^{10}\ \mathrm{cm^6\ mol^{-2}\ s^{-1}}$].

We can, however, simulate the experimental data if we break down the concerted reaction into a subset of reactions, eqns. (15) or (16), (4) and (7) Scheme 4. The reaction mechanism is very sensitive to the rate parameters chosen for eqn. (3), the unimolecular decomposition of $\mathrm{Bu^t{}_2Se}$, *i.e.* the initiation step. The extent of reaction shifts dramatically depending on the value of the activation energy for this step; a change of $+21\ \mathrm{kJ\ mol^{-1}}$ gives rise to virtually no decomposition in the experimental temperature range. The value assigned is the estimate computed from the bond dissociation energy for $\mathrm{Bu^t{}_2Se}$ at the B3LYP/6-311+G(2d,p)//B3LYP/6-311+G(2d,p) level after making thermal corrections appropriate to 298 K.

The identification of critical reaction pathways requires accurate predictions of activation energies; ‘chemical accuracy’ generally refers to errors of 4–8 $\mathrm{kJ\ mol^{-1}}$. It is worthwhile pointing out the likely accuracy of the computed thermochemical kinetic quantities, since a $6\ \mathrm{kJ\ mol^{-1}}$ error in activation energy causes a large uncertainty in k_{298}; a factor of 10. Computed estimates of thermochemical quantities are generally no better than 8–12 $\mathrm{kJ\ mol^{-1}}$ for activation energies (*via* enthalpies of activation) and may well be worse. For entropies the situation is somewhat better, with differences between computed estimates and experimental values typically $<5\%$. This is because an error of even 10% in the vibrational frequencies leads to only a 1% error in the total entropy for a single vibrational degree of freedom for a mode at $200\ \mathrm{cm^{-1}}$ and 300 K. In the present preliminary investigations such a level of accuracy is acceptable.

Further insight into the reaction mechanism can be gained by performing a quasi-stationary state analysis (QSSA) of the free radical mechanism. In particular, chain length of the radical chain has been estimated in order to gauge the importance of possible radical non-chain processes and their dependence on temperature relative to the radical chain. The kinetic chain length λ is defined as the rate of propagation divided by the rate of termination or initiation, since the latter two rates must be equal in the steady state.[60] Hence:

$$\lambda_0 = \frac{k_{\mathrm{obs}}(\mathrm{Bu_2{}^tSe})_0^{3/2}}{k_{\mathrm{i}}(\mathrm{Bu_2{}^tSe})_0} = \frac{k_{\mathrm{obs}}}{k_{\mathrm{i}}}(\mathrm{Bu^t{}_2Se})_0^{1/2} \qquad (1)$$

where $(\mathrm{Bu^t{}_2Se})_0$ is the initial concentration of $\mathrm{Bu^t{}_2Se}$. Using the QSSA computed value for k_{obs} and the estimated values for k_{i} we find that at 700 K (in the middle of the experimental range) λ is *ca.* 3 for pyrolysis in helium but *ca.* 10 for pyrolysis in dihydrogen. Therefore, the approximations made in using a long chain length are valid (a long chain length is generally taken to be $\geqslant 10$)[60] for pyrolysis in dihydrogen but invalid for pyrolysis in helium). It is also important to note that while λ decreases with temperature (from 43 to 5) for pyrolysis in dihydrogen, for pyrolysis in helium λ increases with temperature (from 0.3 to 10). By using the computed values listed in

$$\mathrm{Bu^t{}_2Se} \underset{}{\overset{h\nu}{\rightleftharpoons}} \mathrm{Bu^tSe^\bullet} + \mathrm{Bu^{t\bullet}} \tag{3}$$

$$\mathrm{Bu^tSe^\bullet} \longrightarrow \mathrm{Bu^{t\bullet}} + \mathrm{Se} \tag{4}$$

$$2\,\mathrm{Bu^{t\bullet}} \longrightarrow \mathrm{C_4H_8} + \mathrm{C_4H_{10}} \tag{5}$$

$$2\,\mathrm{Bu^{t\bullet}} \longrightarrow \mathrm{C_8H_{18}} \tag{6}$$

$$\mathrm{Bu^t{}_2Se} + \mathrm{Se} \longrightarrow \mathrm{Bu^t{}_2Se_2} \tag{18}$$

Scheme 5 Proposed mechanism for the photochemical decomposition of $\mathrm{Bu^t{}_2Se}$.

Table 1 it is possible to simulate the experimental results and especially to reproduce the minimal effect of the decomposition profile on changing the carrier gas from He to H_2. These experimental and computed profiles are shown together in Fig. 3. Incorporation of H/D from the carrier gas, H_2 or D_2 into 2-methylpropane is also rationalised because eqn. (14) forms part of the mechanism.

On the basis of the experimental and theoretical observations, we conclude that the reactions occurring during the thermal decomposition of $\mathrm{Bu^t{}_2Se}$ in helium or hydrogen are those shown in Scheme 4.

Photochemical decomposition of $\mathrm{Bu^t{}_2Se}$

There are marked differences in the products and product distributions obtained from thermolysis and photolysis of $\mathrm{Bu^t{}_2Se}$. In particular, the observation that d^9-$\mathrm{Bu^t{}_2Se}$ is produced from photolysis of d^0- and d^{18}-$\mathrm{Bu^t{}_2Se}$ shows that $\mathrm{Bu^tSe^\bullet}$ has a significant lifetime at room temperature when it is generated from $\mathrm{Bu^t{}_2Se}$ by Se–C bond cleavage. This and the remaining observations suggest that radical–radical reactions dominate over H abstraction from intact neutral molecules (Scheme 5). Thus, the near 1 : 1 ratio of 2-methylpropene : 2-methylpropane is as expected for reactions between *tert*-butyl radicals at room temperature [eqn. (5), Scheme 5], as is the appearance of 2,2,3,3-tetramethylbutane.[54] Curiously, $\mathrm{Bu^t{}_2Se_2}$ does not appear to be formed from combination of $2 \times \mathrm{Bu^tSe^\bullet}$ since no d^9-$\mathrm{Bu^t{}_2Se_2}$ is produced when using d^0- and d^{18}-$\mathrm{Bu^t{}_2Se}$. These products presumably arise from a concerted reaction between intact $\mathrm{Bu^t{}_2Se}$ and Se, perhaps photochemically initiated [eqn. (18), Scheme 5]. It is known that for ditellurides, the reverse reaction, the thermal loss of tellurium, does occur by a concerted mechanism [no scrambling of alkyl groups occurs for $\mathrm{RTe_2R'}$ (R, R′ are different alkyls)].[68,69]

Decomposition of $\mathrm{Bu^t{}_2Se}$ in the presence of $\mathrm{Me_2Zn}$

Dimethylzinc has been shown to undergo reversible Zn–C bond cleavage [eqns. (19) and (20), Scheme 6].[70] The products from codecomposing it with $\mathrm{Bu^t{}_2Se}$ are methane and 2-methylpropene with only traces of 2,2-dimethylpropane. We have shown[71] in studies of the codecomposition of $\mathrm{Bu^tTeMe}$ with $\mathrm{Me_2Cd}$ that 2,2-dimethylpropane is a major product if free $\mathrm{Bu^{t\bullet}}$ and $\mathrm{Me^\bullet}$ are generated together. This means that few if any free $\mathrm{Bu^{t\bullet}}$¶ are generated during the codecomposition of $\mathrm{Me_2Zn}$ and $\mathrm{Bu^t{}_2Se}$, and hence that a mechanism similar to that of Scheme 4, but with initiation of the chain reaction by $\mathrm{Me^\bullet}$ abstracting H from intact $\mathrm{Bu^t{}_2Se}$ cannot be operating. However, the labelling pattern for the products from $\mathrm{Me_2Zn}$ and d^{18}-$\mathrm{Bu^t{}_2Se}$ in helium, d^1-methane and d^8-2-methylpropene suggest that H abstraction by Me radicals must be occurring. The presence of methyl radicals is also suggested by the observation that the methane produced in the codecomposition of $\mathrm{Me_2Zn}$ and d^{18}-$\mathrm{Bu^t{}_2Se}$ in hydrogen is largely CH_4, formed by the reaction of $\mathrm{Me^\bullet}$ with H_2. Gorochov and coworkers have shown that the decomposition temperature of $\mathrm{Bu^t{}_2Se}$ is reduced by 200 °C if the studies are carried out in a tube coated with ZnSe, compared with a glass tube.[25] This is clear evidence that surface catalysed processes are important for the decompositions carried out in the presence of ZnSe and hence for the codecomposition reactions. If the reaction occurs on the surface, reactions such as (12) or (13) in Scheme 3 should become thermodynamically accessible since surface bound Se and H are formed rather than the high energy species, $\mathrm{Se_{(g)}}$ and $\mathrm{H^\bullet{}_{(g)}}$. All of the observations for the codecomposition of $\mathrm{Me_2Zn}$ with $\mathrm{Bu^t{}_2Se}$ can then be explained as shown in Scheme 6, with all the reactions occurring on the surface. $\mathrm{Me^\bullet}$ abstracts $\mathrm{H^\bullet}$ from surface bound $\mathrm{Bu^t{}_2Se}$, as in eqn. (21), Scheme 6, to produce methane, $2 \times$ 2-methylpropene, adsorbed Se atoms and $\mathrm{H_{(ads)}}$, which then starts a chain reaction [eqn. (13), Scheme 6], from which the products are H_2, $\mathrm{Se_{(ads)}}$ and 2-methylpropene. The labelled products are the expected CH_3D and d^8-2-methylpropene if d^{18}-$\mathrm{Bu^t{}_2Se}$ is used in place of d^0-$\mathrm{Bu^t{}_2Se}$. Hydrogen is incorporated into the methane from the carrier gas (H_2) through eqn. (22), Scheme 6. The 2-methylpropane formed if the reaction is carried out in hydrogen or deuterium must arise from a sequential hydrogenation of 2-methylpropene [eqn. (24), Scheme 6] since it contains 2H from the carrier gas (d^2- from d^0-$\mathrm{Bu^t{}_2Se}$ in D_2 or d^8- from d^{18}-$\mathrm{Bu^t{}_2Se}$ in H_2). This also accounts for the increased formation of 2-methylpropane at higher temperature. Presumably, ZnSe catalyses the hydrogenation reaction, since this reaction is not observed in the absence of zinc.

$$\mathrm{Me_2Zn_{(ads)}} \rightleftharpoons \mathrm{MeZn^\bullet{}_{(ads)}} + \mathrm{Me^\bullet{}_{(ads)}} \tag{19}$$

$$\mathrm{MeZn^\bullet{}_{(ads)}} \longrightarrow \mathrm{Zn_{(ads)}} + \mathrm{Me^\bullet{}_{(ads)}} \tag{20}$$

$$\mathrm{Me^\bullet{}_{(ads)}} + \mathrm{Bu^t{}_2Se_{(ads)}} \longrightarrow \mathrm{CH_4} + 2\,\mathrm{C_4H_8} + \mathrm{Se_{(ads)}} + \mathrm{H^\bullet{}_{(ads)}} \tag{21}$$

$$\mathrm{H^\bullet{}_{(ads)}} + \mathrm{Bu^t{}_2Se_{(ads)}} \longrightarrow \mathrm{H_2} + 2\,\mathrm{C_4H_8} + \mathrm{Se_{(ads)}} + \mathrm{H^\bullet{}_{(ads)}} \tag{13}$$

$$\mathrm{Me^\bullet{}_{(ads)}} + \mathrm{H_2} \longrightarrow \mathrm{CH_4} + \mathrm{H^\bullet{}_{(ads)}} \tag{22}$$

$$\mathrm{Me^\bullet{}_{(ads)}} + \mathrm{H^\bullet{}_{(ads)}} \longrightarrow \mathrm{CH_4} \tag{23}$$

$$2\,\mathrm{H^\bullet{}_{(ads)}} \longrightarrow \mathrm{H_2} \tag{8}$$

$$\mathrm{C_4H_8} + \mathrm{H_2} \xrightarrow{\mathrm{ZnSe}} \mathrm{C_4H_{10}} \tag{24}$$

Scheme 6 Proposed mechanism for the growth of ZnSe by MOVPE using $\mathrm{Bu^t{}_2Se}$ and $\mathrm{Me_2Zn}$.

Conclusions

A detailed study of the products obtained from thermal decomposition of deuterium labelled and unlabelled $\mathrm{Bu^t{}_2Se}$ has allowed us to show that the decomposition proceeds by initial Se–C bond cleavage. $\mathrm{Bu^tSe^\bullet}$ is not stable under thermal reaction conditions but decomposes *via* a second Se–C bond cleavage. The $\mathrm{Bu^{t\bullet}}$ formed lose $\mathrm{H^\bullet}$ or react with intact $\mathrm{Bu^t{}_2Se}$ initiating a chain reaction to give 2-methylpropane, $2 \times$ 2-methylpropene, Se and $\mathrm{H^\bullet}$, which then acts as the chain carrier. In the presence of $\mathrm{Me_2Zn}$, the radical chain initiator is $\mathrm{Me^\bullet}$, but the chain is still carried by $\mathrm{H^\bullet}$. Although Se–H bonds are not formed in the decomposition of $\mathrm{Bu^t{}_2Se}$, nor in its reaction with $\mathrm{Me_2Zn}$, the fact that the chain carrier in the decomposition is $\mathrm{H^\bullet}$ means that passivation of *e.g.* N dopants may still be a significant problem in achieving active doping with nitrogen. Photochemical initiation of the decomposition of $\mathrm{Bu^t{}_2Se}$ again proceeds by a free radical process, but this time neither Se–H nor $\mathrm{H^\bullet}$ are produced so this may present a better method for obtaining active N doping in ZnSe.

Acknowledgements

We thank the EPSRC for Fellowships (N.L.P., D.F.F.).

¶ At the temperature of the codecomposition reactions (≪400 °C), $\mathrm{Bu^{t\bullet}}$ is stable towards loss of $\mathrm{H^\bullet}$.[54]

References

1 D. N. Armitage, H. M. Yates, J. O. Williams, D. J. Cole-Hamilton and I. L. J. Patterson, *Adv. Mater. Opt. Electron.*, 1992, **1**, 43.

2 D. F. Foster, I. L. J. Patterson, L. D. James, D. J. Cole-Hamilton, D. N. Armitage, H. M. Yates, A. C. Wright and J. O. Williams, *Adv. Mater. Opt. Electron*, 1994, **3**, 163.

3 M. Danek, J. S. Huh, L. Foley and K. F. Jensen, *J. Cryst. Growth*, 1994, **145**, 530.

4 K. Nishimura, Y. Nagato and K. Sakai, *Jpn. J. Appl. Phys.*, 1993, **32**, L428.

5 W. S. Kuhn, A. Naumov, H. Stanzl, S. Bauer, K. Wolf, H. P. Wagner, E. Gebhardt, U. W. Pohl, A. Krost, W. Richter, U. Dumichen and K. H. Thiele, *J. Cryst. Growth*, 1992, **123**, 605.

6 B. Bollig, M. Blauermel, W. Taudt and M. Henken, *J. Cryst. Growth*, 1994, **145**, 562.

7 W. Taudt, B. Wachtendorf, R. Beccard, A. Wahid, M. Henken, A. L. Gurskii and K. Vakarelska, *J. Cryst. Growth*, 1994, **145**, 582.

8 T. Obinata, K. Vesugi, G. Sato, I. Suemune, H. Machida and N. Shimoyama, *Jpn. J. Appl. Phys.*, 1995, **34**, 4143.

9 W. S. Kuhn, R. Driad, H. Stanzl, A. Lusson, K. Wolf, B. Qu'Hen, H. Sahin, L. Srob, C. Grattepain, X. Quesada, W. Grebhardt and O. Gorochov, *J. Cryst. Growth*, 1994, **138**, 448.

10 K. Wolf, H. Stanzl, A. Naumov, H. P. Wagner, W. S. Kahn, B. Hahn and W. Gebhardt, *J. Cryst. Growth*, 1994, **138**, 412.

11 P. J. Wright, B. Cockayne, P. J. Parbrook, P. E. Oliver and A. C. Jones, *J. Cryst. Growth*, 1991, **108**, 525 and references therein.

12 N. L. Pickett, D. F. Foster and D. J. Cole-Hamilton, *J. Mater. Chem.*, 1996, **6**, 507.

13 N. L. Pickett, D. F. Foster and D. J. Cole-Hamilton, *J. Cryst. Growth*, 1997, **170**, 476.

14 N. L. Pickett, F. G. Riddell, D. F. Foster, D. J. Cole-Hamilton and J. R. Fryer, *J. Mater. Chem.*, 1997, **8**, 1855.

15 A. Kamata, M. Mitsuhashi and H. Fujita, *Appl. Phys. Lett.*, 1993, **63**, 3353.

16 N. L. Pickett, D. F. Foster, W. G. Thomas, F. G. Riddell, D. J. Cole-Hamilton and J. R. Fryer, *J. Mater. Chem.*, 1998, **8**, 2769.

17 H. Bock and S. Mohmand, *Angew. Chem., Int. Ed. Engl.*, 1977, **16**, 104.

18 G. Martin and N. Barroeta, *Int. J. Chem. Kinet.*, 1980, **12**, 699.

19 T. Hirabayashi, S. Mohmand and H. Bock, *Chem., Ber.*, 1982, **115**, 483.

20 C. G. Thompson, R. A. Mayer and J. S. Ball, *J. Am. Chem. Soc.*, 1952, **74**, 3284.

21 W. Tsang, *J. Chem. Phys.*, 1964, **40**, 1498.

22 T. Bamkole, *J. Chem. Soc., Perkin Trans. 2*, 1977, 439.

23 M. Sugioka, T. Yotsuyangi and K. Aomura, *Hokkaido Daigaku Kugakuba Kenkyu Hokoku*, 1970, **57**, 191; *Chem. Abstr.*, 1973, **78**, 29000w.

24 M. Yamada, T. Kamo, J. Tang, Y. Oshima and A. Amano, *Nippon Kagaku Kaishi*, 1985, 2283; *Chem. Abstr.*, 1986, **104**, 224462f.

25 W. S. Kuhn, R. Helbing, B. Qu'Hen and O. Gorochov, *J. Cryst. Growth*, 1995, **146**, 580.

26 G. H. Fan, N. Maung, T. L. Ng, P. F. Heelis, J. O. Williams, A. C. Wright, D. F. Foster and D. J. Cole-Hamilton, *J. Cryst. Growth*, 1997, **170**, 485.

27 W. Bell, J. Stevenson, D. J. Cole-Hamilton and J. E. Hails, *Polyhedron*, 1994, **13**, 1253.

28 N. L. Pickett, D. F. Foster, D. J. Cole-Hamilton and J. E. Hails, *Phosphorus Sulphur Silicon*, 1998, **136–138**, 427.

29 N. L. Pickett, D. F. Foster and D. J. Cole-Hamilton, in *Fundamental Gas-phase and Surface Chemistry of Vapour-phase Synthesis*, eds. M. D. Allendorf, M. R. Zachariah, L. Mountziaris and A. H. McDaniel, Electrochemical Society Proceedings, Pennington, 1999, vol. 98–23, p. 307.

30 D. F. Foster and D. J. Cole-Hamilton, *Inorg. Synth.*, 1997, **31**, 29.

31 D. F. Foster, N. L. Pickett and D. J. Cole-Hamilton, *Polyhedron*, 1999, **18**, 1329.

32 R. C. Morrison, R. W. Hall, J. A. Schwindeman, C. W. Kamienski and J. F. Engel, *US Pat.*, 5340507, 1994.

33 R. C. Morrison, R. W. Hall, J. A. Schwindeman, C. W. Kamienski and J. F. Engel, *Eur. Pat. Appl.*, 0525881Al, 1993.

34 L. D. Stockton, T. L. Ng, N. Maung, I. B. Poole, J. O. Williams, A. C. Wright, D. F. Foster and D. J. Cole-Hamilton, *J. Cryst. Growth*, 1998, **183**, 95.

35 W. J. Hehre, L. Radom, P. R. v. Schleyer and J. A. Pople, *Ab Initio Molecular Orbital Theory*, John Wiley and Sons, New York, 1986.

36 R. G. Parr and Y. Weitao, *Density-Functional Theory of Atoms and Molecules*, Oxford University Press, Oxford, 1995.

37 J. M. Seminario and P. Politzer, *Modern Density Functional Theory: A Tool for Chemistry*, Elsevier, Amsterdam, 1995.

38 N. Maung, J. O. Williams and A. C. Wright, *J. Mol. Struct. (THEOCHEM)*, 1998, **453**, 181.

39 GAUSSIAN 94 (Revision E.1), M. J. Frisch, G. W. Trucks, H. B. Schlegel, P. M. W. Gill, B. C. Johnson, M. A. Robb, J. R. Cheeseman, T. A. Keith, G. A. Petersson, J. A. Montgomery, K. Raghavachari, M. A. Al-Laham, V. G. Zakrzewski, J. V. Ortiz, J. B. Foresman, J. Cioslowski, B. B. Strefanov, A. Nanayakkara, M. Challacombe, C. Y. Peng, P. Y. Ayala, W. Chen, M. W. Wong, J. L. Andres, E. S. Replogle, R. Gomperts, R. L. Martin, D. J. Fox, J. S. Binkley, D. J. Defrees, J. Baker, J. P. Stewart, M. Head-Gordon, C. Gonzalez and J. A. Pople, Gaussian Inc., Pittsburgh, PA, 1995.

40 SPARTAN version 4.1.2, Wavefunction Inc., 18401 Von Karman Ave., #370, Irvine, CA92715, USA, ©1995 Wavefunction, Inc.

41 W. J. Hehre, L. D. Burke, A. J. Shusterman and W. J. Pietro, *Experiments in Computational Organic Chemistry*, Wavefunction, Inc. Irvine, 1993.

42 W. J. Hehre, *Practical Strategies for Electronic Structure Calculations*, Wavefunction, Inc. Irvine, CA, 1995.

43 W. J. Hehre, A. J. Shusterman and W. W. Huang, *A Laboratory Book of Computational Organic Chemistry*, Wavefunction, Inc. Irvine, CA, 1996.

44 *Gaussian 94 (Revision D.1 and higher) User's Reference*, Gaussian Inc., Pittsburgh, PA, 1994–1996.

45 J. B. Foresman and A. E. Frisch, *Exploring Chemistry with Electronic Structure Methods*, Gaussian Inc., Pittsburgh, PA, 2nd edn., 1995–96.

46 J. J. P. Stewart, MOPAC 93, Fujitsu Limited, Tokyo, Japan, 1993.

47 J. J. P. Stewart, *J. Comput. Chem.*, 1989, **10**, 209.

48 M. J. S. Dewar and W. J. Thiel, *J. Am. Chem. Soc.*, 1977, **99**, 4899.

49 M. J. S. Dewar, E. G. Zoebisch, E. F. Healy and J. J. P. Stewart, *J. Am. Chem. Soc.*, 1985, **107**, 3902.

50 T. A. Halgren and W. N. Lipscomb, *Chem. Phys. Lett.*, 1977, **49**, 225.

51 W. H. Press, S. A. Teukolsky, W. T. Vetterling and B. P. Flannery, *Numerical Recipes in FORTRAN–The Art of Scientific Computing*, Cambridge University Press, Cambridge, 1992.

52 Mathcad 6.0, Mathsoft Inc., 1996.

53 N. L. Pickett, D. F. Foster and D. J. Cole-Hamilton unpublished observations.

54 R. N. Birrell and A. F. Trotman-Dickenson, *J. Chem. Soc.*, 1960, 4218.

55 W. K. An, M. J. Kappers and R. F. Hicks, *J. Cryst. Growth*, 1997, **173**, 386.

56 J. Stevenson, W. Bell, J. Ferry. D. J. Cole-Hamilton and J. E. Hails, *J. Organomet. Chem.*, 1993, **449**, 141.

57 N. Maung, J. O. Williams and A. C. Wright, *Chem. Mater.*, 1999, submitted for publication.

58 S. W. Benson, *J. Chem. Soc., Faraday Trans. 2*, 1987, **83**, 791.

59 S. W. Benson, *Chem. Rev.*, 1978, **78**, 23.

60 S. W. Benson, *Thermochemical Kinetics*, John Wiley & Sons, New York, 1976.

61 D. F. Foster, C. Glidewell, G. R. Woolley and D. J. Cole-Hamilton, *J. Electron. Mater.*, 1995, **24**, 1731.

62 W. Tsang, *J. Phys. Chem. Ref. Data*, 1990, **19**, 1.

63 V. D. Knyazev, I. A. Dubinsky, I. R. Slagle and D. Gutman, *J. Phys. Chem.*, 1994, **98**, 5279.

64 W. Tsang and R. F. Hampson, *J. Phys. Chem. Ref. Data*, 1986, **15**, 1087.

65 J. V. Michael and J. R. Fisher, *J. Phys. Chem.*, 1990, **94**, 3318.

66 J. V. Michael, *J. Chem. Phys.*, 1990, **92**, 3394.

67 J. I. Steinfield, J. S. Francisco and W. L. Hase, *Chemical Kinetics and Dynamics*, Prentice-Hall, Englewood Cliffs, NJ, 1989.

68 A. E. D. McQueen, M. B. Parker, J. B. Mullin and D. J. Cole-Hamilton, *Chemtronics*, 1989, **4**, 264.

69 A. E. D. McQueen, P. N. Culshaw, J. C. Walton. D. V. Shenai-Khatkhate, D. J. Cole-Hamilton and J. B. Mullin, *J. Cryst. Growth*, 1991, **107**, 325.

70 J. E. Hails and D. J. Cole-Hamilton, unpublished observations.

71 J. E. Hails, D. J. Cole-Hamilton and A. E. D. McQueen, *J. Crystal Growth*, 1998, **183**, 594.

Paper 9/04270I